THE JOURNAL OF PHYSICAL CHEMISTRY C
A JOURNAL OF THE AMERICAN CHEMICAL SOCIETY

pubs.acs.org/JPCC

Article

Highly Efficient Triplet–Triplet Annihilation Upconversion with a Thermally Activated Delayed Fluorescence Molecule as Triplet Photosensitizer

Min Zheng, Yuanming Li, Yaxiong Wei,* Lin Chen,* Shilin Liu, and Xiaoguo Zhou*

Cite This: *J. Phys. Chem. C* 2023, 127, 2846–2854

Read Online

ACCESS | Metrics & More | Article Recommendations | Supporting Information

ABSTRACT: Thermally activated delayed fluorescence (TADF) molecules have great potential for practical applications as triplet photosensitizers, owing to their long triplet lifetimes, almost negligible energy loss in intersystem crossing, and excellent light-harvesting ability. Recently, several triplet–triplet annihilation (TTA) upconversion systems using the TADF photosensitizer have been reported. To provide comprehensive dynamic information for designing an optimized system in the future, more experiments with the new TADF photosensitizers are necessary. Herein, we conducted a new TTA upconversion system with a recently developed TADF molecule, DMACPDO, as the triplet photosensitizer and 9,10-diphenylanthracene (DPA) as the annihilator. The overall upconversion yield was determined to be relatively high, e.g., 22.3% in toluene, 21.9% in benzene, and 8.1% in chlorobenzene. By examining elementary photophysical and photochemical processes with time-resolved transient absorption and fluorescence emission spectroscopy, we revealed the influence of solvent polarity and viscosity on each step. Our conclusion highlights the elusive solvent effect in TTA upconversion application of the TADF photosensitizer.

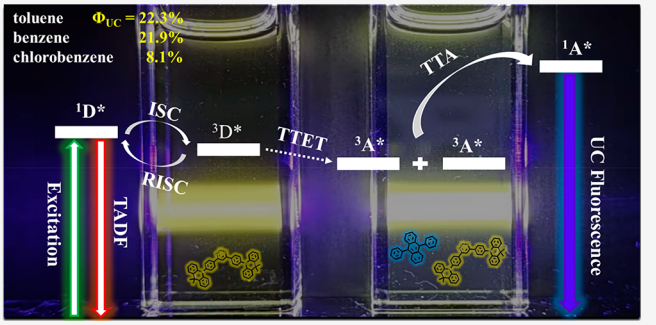

1. INTRODUCTION

Photon upconversion is one of the most important methods to further improve the efficiency for single heterojunction organic solar cells, in which light of long wavelength is frequency-converted to photons of higher energy. Since Parker and Hatchard first reported TTA upconversion in the 1960s,[1] TTA upconversion has attracted extensive attention due to its advantages like low excitation power density requirement, high quantum yield, and tunable anti-Stokes shift.[2−8] To date, TTA upconversion has been successfully applied in photovoltaics,[9−11] photocatalytics,[12,13] biological imaging,[14−16] and photodynamic therapy.[17,18]

A TTA upconversion system usually consists of one photosensitizer (energy donor) and an annihilator (energy acceptor). After absorbing light, the photosensitizer usually undergoes intersystem crossing (ISC) and a bimolecular triplet–triplet energy transfer (TTET) to form a triplet annihilator; then upconversion fluorescence can be observed from the excited singlet annihilator produced by the TTA of two triplet annihilators.[19] To achieve the higher upconversion efficiency, photosensitizers should have a high molar extinction coefficient, an efficient ISC ability, and a long-lived triplet state. In previous studies, most of photosensitizers are those complexes containing transition metals such as Pt(II), Ru(II), and Ir(II)[7,20−25] or heavy atoms like I and Br.[4,26−29] Because of the heavy-atom effect, spin–orbit coupling is enhanced to efficiently produce the triplet manifold.[7] However, the practical application of these heavy-atom-containing photosensitizers has some drawbacks, such as biological cytotoxicity, environmental pollution, and high cost. Therefore, development of heavy-atom-free organic triplet photosensitizers is the most fascinating project related to TTA upconversion. In recent years, a series of BODIPY derivatives have been successfully designed and applied as light-harvesting triplet energy donors to achieve TTA upconversion.[11,27,28,30] Compared with those traditional heavy-atom-free organic photosensitizers like BODIPY derivatives, an organic TADF molecule not only has a long-lived triplet state, but also its small singlet–triplet energy gap (ΔE_{S-T} < 100 meV)[31] offers the possibility of minimizing energy loss in the ISC process. These advantages lead to a conception that TADF molecules are potential photosensitizers. So far, some successful applications of TADF photosensitizer on TTA upconversion have been reported recently.[32−38] The first example was shown by Baldo and colleagues with the 4-CzTPN-Ph/DPA (photosensitizer/

Received: November 9, 2022
Revised: January 24, 2023
Published: February 3, 2023

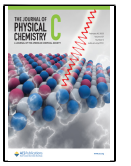

https://doi.org/10.1021/acs.jpcc.2c07906
J. Phys. Chem. C 2023, 127, 2846–2854

annihilator) bilayer film.[39] Although the upconverted light from green (532 nm) to blue (420 nm) was observed, a low upconversion quantum yield (Φ_{UC}) of 0.28% was unsatisfactory due to inefficient TTET process. By covalently linking a TADF molecule (4CzIPN) with an annihilator (DBP), Peng et al. overcame this shortcoming and enhanced the upconversion fluorescence by 80-fold compared to the system of isolated 4CzIPN and DBP.[33] In 2019, Song et al. observed red-to-blue photon upconversion in solution with a TADF photosensitizer for the first time, and a 207 nm anti-Stokes shift and a high Φ_{UC} of 11.2% were achieved.[36] Very recently, Albinsson and co-workers reported a visible-to-ultraviolet photon upconversion system, in which a record-setting internal quantum yield ($\Phi_{UC,g}$ = 33.6% with a 100% maximum) was determined to approach the spin-statistical limit.[38] By pairing a multiple resonance TADF photosensitizer (BN-2Cz-tBu) with the annihilator (1,5-DTNA), we also realized green-to-ultraviolet TTA upconversion in solution with an anti-Stokes shift up to 1.05 eV, the Φ_{UC} value of 8.6%, and the threshold excitation power as low as 9.2 mW cm^{-2}.[37] These examples fully demonstrate the potential of the TADF molecules as the photosensitizer for TTA upconversion.

In a TTA upconversion system with the TADF photosensitizer (Figure 1), three competitive kinetic pathways coexist for the triplet TADF molecule, i.e., reverse ISC (RISC), nonradiation to the ground state, and TTET to the annihilator. In the case of extremely small ΔE_{S-T}, the RISC might be dominant rather than the bimolecular TTET, and as a result, the TTA upconversion efficiency is low. Thus, a moderate ΔE_{S-T} facilitates balancing this competition in the TTA upconversion dynamics.[38] Moreover, as a bimolecular Dexter energy transfer process, the TTET rate is solvent-dependent as the diffusion rate and the triplet lifetime vary with the viscosity of the solvent,[4] and solvent viscosity probably has a considerable influence on the TTA efficiency.[40] Additionally, the ΔE_{S-T} value is significantly varied by solvent polarity, as observed recently in TADF molecules.[41] Therefore, revealing the elusive solvent effect in the overall TTA upconversion process is of great significance for the application of TADF photosensitizers.

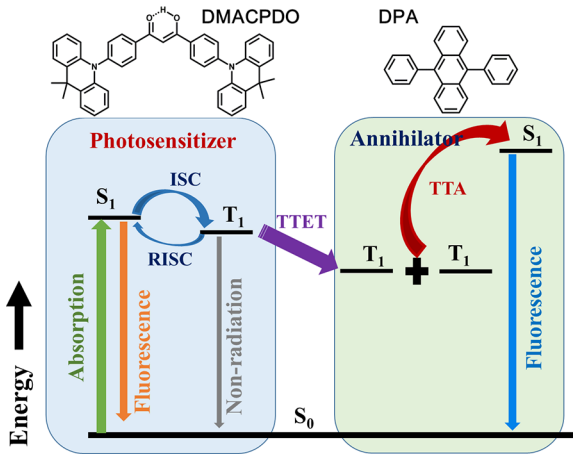

Figure 1. Jablonski diagram illustrating the TTA upconversion process between a TADF photosensitizer and an annihilator, where ISC and RISC are intersystem crossing and its reverse process, TTET represents triplet-to-triplet energy transfer, and TTA is triplet−triplet annihilation.

In this work, we conducted a new TTA upconversion system with a recently reported TADF molecule, DMACPDO,[42] as the photosensitizer and DPA as the annihilator. The time-resolved transient absorption and fluorescence emission spectra were measured in three common solvents, toluene, benzene and chlorobenzene. By comparing the obtained quantum yields of ISC, TTET and fluorescence emission of DPA, as well as the overall upconversion quantum efficiency, the complex influence of solvent polarity and viscosity was discussed.

2. EXPERIMENTS AND COMPUTATIONS

DMACPDO was synthesized according to the previous literature.[42] All the precursors were analytically pure and were purchased from Sigma-Aldrich Co. and used without any purification. To avoid self-quenching of photosensitizer in a high concentration, a relatively low DMACPDO concentration (1×10^{-5} M) was chosen in following experiments, and three solvents, i.e., toluene, benzene, and chlorobenzene, were used. The solutions were deoxygenated by purging with high-purity argon (99.99%) for at least 20 min prior to measurements.

Nanosecond time-resolved transient absorption and delayed fluorescence emission spectra were measured with the home-built laser flash photolysis system and the fluorescence emission spectrometer.[43,44] Briefly, the third harmonic (355 nm) of a Q-switched Nd:YAG laser (Dawa-100, Beamtech) was used as the excitation light source (8 ns, 10 Hz, ~10 mJ/pulse). In the transient absorption measurements, an analyzing light from a 500 W xenon lamp and the pulsed laser passed through a quartz cuvette (10 mm × 10 mm) perpendicularly. A

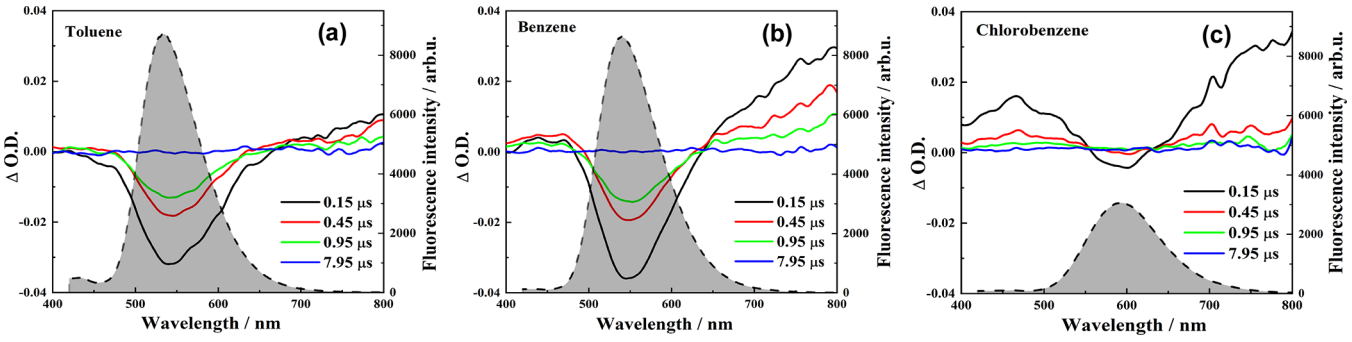

Figure 2. Nanosecond time-resolved transient absorption spectra (solid lines) of DMACPDO (1×10^{-5} M) in deoxygenated toluene, benzene, and chlorobenzene at room temperature and λ_{ex} = 355 nm as well as the fluorescence emission spectra (dotted lines) of DMACPDO (1×10^{-5} M) in deoxygenated solvents at room temperature and λ_{ex} = 405 nm.

https://doi.org/10.1021/acs.jpcc.2c07906
J. Phys. Chem. C 2023, 127, 2846−2854

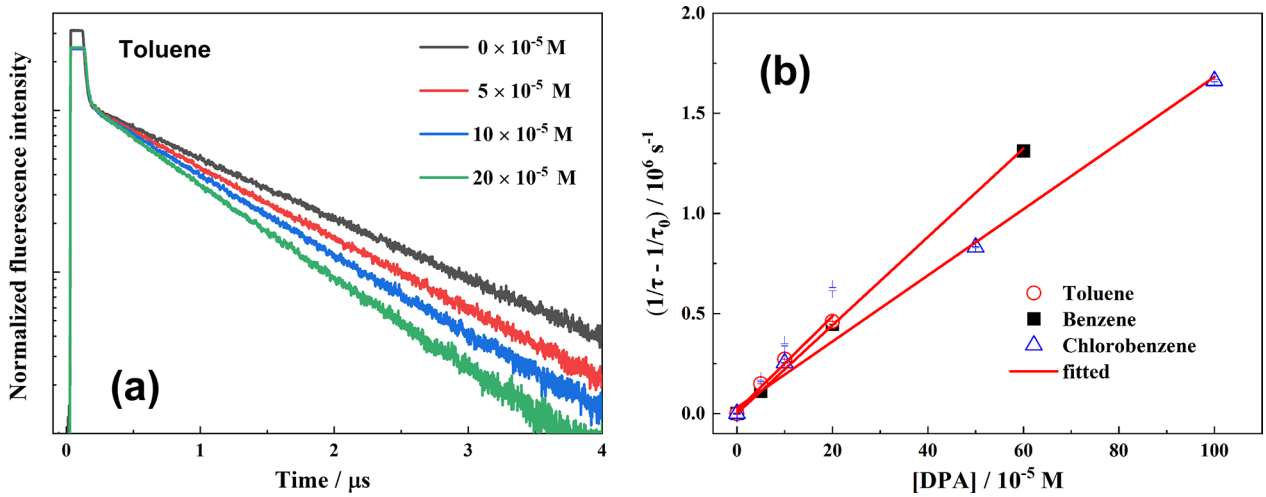

Figure 3. (a) Fluorescence emission kinetics for DMACPDO (1×10^{-5} M) in the presence of DPA with various concentrations in deoxygenated toluene at room temperature and λ_{ex} = 355 nm. (b) Stern−Volmer plots generated from the delayed fluorescence quenching of DMACPDO (1×10^{-5} M) in the presence of DPA in the three solvents.

monochromator equipped with a photomultiplier (CR131, Hamamatsu) was utilized to measure the transient spectra within the wavelength range of 400−800 nm, and the kinetic data were recorded with an oscilloscope (TDS3052B, Tektronix). Time-dependent fluorescence emission dynamics were measured using a spectrometer (FluoTime 300, PicoQuant) with a picosecond pulsed laser (LASER375, PicoQuant) as the photoexcitation source.

A semiconductor laser at 455 nm was used as the excitation light source in the TTA upconversion experiment. The diameter of the laser spot in sample region was ∼3.5 mm. The mixed solution of DMACPDO and DPA was deoxygenated by purging with argon for at least 20 min, and the gas flow was kept during measurements. Fluorescence emission was collected and analyzed with a commercial fiber-optic spectrometer (AvaSpec-ULS2048, Avantes). The spectral resolution was ∼0.5 nm.

3. RESULTS AND DISCUSSION

3.1. Nanosecond Transient Absorption Spectra. Figure 2 shows the nanosecond time-resolved transient absorption spectra of DMACPDO in the three solvents with photoexcitation at 355 nm at the delay times of 0.15−7.95 μs. One negative peak (500−650 nm) and two positive absorption bands (400−500 nm and 650−800 nm) are generally observed in these spectra. Their intensities are changed in different solvents, and moreover, the peak position of the negative band shows a distinct red-shift, i.e., 540 nm in toluene, 550 nm in benzene, and 600 nm in chlorobenzene. It is worth noting that there are significant variations with both intensity and position of fluorescence emission peak (dotted lines in Figure 2) in the three solvents, although the lowest-energy absorption peak in steady-state absorption spectrum of DMACPDO is maintained at the same range of 400−500 nm with approximate intensity (Figure S1 of the Supporting Information). According to the fact that the strong negative transient absorption peak in Figure 2 is exactly located at the fluorescence emission wavelength range in each solvent, the band at 500−650 nm can be readily assigned to the stimulated emission of DMACPDO. Moreover, its decay rate is consistent with the reciprocal of the reported delayed fluorescence lifetime of DMACPDO.[41] In addition, the intensity of this negative peak shows a consistent trend with fluorescence intensity, providing further evidence for the spectral assignment of stimulated emission.

Two positive absorption bands are observed in Figure 2 at 400−500 and 650−800 nm. Notably, this higher-energy band is located in the lowest-energy absorption peak range of DMACPDO, where a negative ground-state bleaching (GSB) band usually exists. Thus, the positive absorption of the triplet state (visible in chlorobenzene and benzene) and the negative GSB counteract with each other, resulting in its weak intensity in the transient absorption spectra. Especially in toluene, this competition almost neutralizes the corresponding triplet absorption. The second wide and positive absorption band at 650−800 nm can be readily assigned to the absorption of triplet DMACPDO. This conclusion can be also confirmed by their decay rates close to the reciprocal of delayed fluorescence lifetime of DMACPDO in the same solvent.[41] On the basis of this consistence, we used the decay lifetime of stimulated emission at 500−600 nm to represent the lifetime of triplet DMACPDO owing to its better signal-to-noise ratio and performed the kinetic measurements of the energy transfer between triplet DMACPDO and annihilator.

3.2. Triplet−Triplet Energy Transfer from DMACPDO to DPA. Upon being excited, fluorescence emission of a TADF molecule usually includes a simultaneous prompt fluorescence component with a short lifetime (picoseconds to a few tens of nanoseconds) and a delayed fluorescence component with a long lifetime (microseconds), where the latter arises from the thermally activated RISC from nearby triplet states. Apparently, the obvious lifetime of delayed fluorescence is related to the quenching by annihilators, while the prompt fluorescence component is not concerned. Thus, in Figure 3a we show the delayed fluorescence kinetics of DMACPDO in the presence of DPA in different concentrations. Apparently, the lifetime of delayed fluorescence is gradually reduced with the addition of DPA, indicative of an efficient TTET between triplet DMACPDO and DPA. According to the Stern−Volmer equation, $1/\tau = 1/\tau_0 + k_{TTET}[DPA]$, where τ and τ_0 are the lifetimes in the presence and absence of DPA; the bimolecular TTET rate constant, k_{TTET}, can be achieved by fitting the observed lifetime of delayed fluorescence as a function of the DPA concentration, as shown in Figure 3b.

https://doi.org/10.1021/acs.jpcc.2c07906
J. Phys. Chem. C 2023, 127, 2846−2854

Table 1 lists the obtained TTET rate constants and the calculated diffusion rates $k_{diffuse}$ (= $8k_BT/3\eta$) in the three solvents, where η is the viscosity of the solvent. Apparently, the k_{TTET} value shows the same subsequence with the predicted $k_{diffuse}$ in the all solvents. However, it is worth noting that the experimental data are all only ~1/5 of the theoretical values in the solvents, implying that the TTET process is not completely controlled by diffusion. Using k_{ET} to denote the energy transfer rate constant for an encounter of (^{3}DA) in a solvent cage, we can simply calculate the overall k_{TTET} value by $k_{TTET} = k_{diffuse}\frac{k_{ET}}{k_{diffuse}+k_{ET}}$. Given $k_{TTET} = k_{diffuse}/5$, the k_{ET} value approximately equals $k_{diffuse}/4$ and decreases along the sequence of toluene, benzene, and chlorobenzene. It is well-known that as a typical Dexter mechanism, the rate constant of exchange energy transfer is theoretically given by $k_{Dexter} = KJ\exp(-2R_{DA}/L)$, where J is the normalized spectral overlap integral, K is an experimental factor, R_{DA} is the distance between donor and acceptor, and L is the sum of the van der Waals radius. For the Dexter energy transfer from triplet DMACPDO to DPA, K, R_{DA}, and L are all constant in the solvents. As discussed in Section 3.4, the energies and frontier molecular orbits of the lowest triplet states of DMACPDO and DPA are virtually unchanged in the three solvents. Hence, the J value remains due to identical spectral overlap, and the approximate k_{Dexter} values can be expected. Given this, the contribution of the RISC process should play a crucial role for the phenomenological variation of k_{TTET} because the competition between RISC and bimolecular TTET processes could affect the branching ratio of energy transfer for the ^{3}DA encounter.

Table 1. Bimolecular TTET Rate Constants (k_{TTET}) between the Triplet DMACPDO and DPA

solvent	η (cP)	ε	k_{TTET} ($\times 10^9$ M^{-1} s^{-1})	$k_{diffuse}$ ($\times 10^9$ M^{-1} s^{-1})
toluene	0.59	2.240	2.36 ± 0.20	11.3
benzene	0.60	2.283	2.20 ± 0.02	11.1
chlorobenzene	0.80	5.649	1.65 ± 0.14	8.3

As we reported recently,[41] ΔE_{S-T} of DMACPDO is 0.11 ± 0.01 eV in toluene and 0.10 ± 0.01 eV in benzene. Using the identical strategy, this value is determined to be 0.08 ± 0.01 eV in chlorobenzene. Thus, with increasing the solvent polarity, the decreased ΔE_{S-T} can accelerate the RISC rate and reduce the delayed fluorescence lifetime as we observed in experiments,[41] e.g., 1039 ns in toluene, 1100 ns in benzene, and 605 ns in chlorobenzene. Apparently, the increased RISC rate will naturally reduce the TTET efficiency in polar solvent compared with the unchanged k_{Dexter} value.

Notably, when we use a high enough concentration of DPA as 10 mM as below, it is much higher than that of DMACPDO. With the pseudo-first-order approximation, the estimated k_{TTET}[DPA] (~2 × 10^7 s^{-1}) is much larger than k_{RISC} (~3 × 10^5 s^{-1} from ref 41). Then, the obtained TTET efficiency (Φ_{TTET}) is close to unity according to eq 1:

$$\Phi_{TTET} = k_{TTET}[DPA]/(k_{TTET}[DPA] + k_{RISC} + k_{NR}^T) \quad (1)$$

where k_{NR}^T represents the rate constant of nonradiation pathways for triplet DMACPDO. As reported previously,[41] the k_{NR}^T value is ca. 6 × 10^5 s^{-1} and is negligible relative to k_{TTET}[DPA]. In this case, the solvent effect can be ignored for the TTET process.

3.3. TTA Upconversion Fluorescence Emission of DPA. With excitation at 455 nm, only fluorescence emission from DMACPDO itself was observed within the range of 470−630 nm in the absence of DPA, as shown in the black trace of Figure 4a. With the addition of DPA, a new and strong fluorescence emission appeared in the range of 405−470 nm, besides the original luminescence. This spectral profile is identical with the fluorescence spectrum of DPA itself with excitation at 355 nm, indicating an occurrence of upconversion fluorescence emission. As shown in Figure 4a, this fluorescence intensity gradually increases with the DPA concentration. However, the blue-side fluorescence peak at ~415 nm of DPA gradually disappears with the increase of the DPA concen-

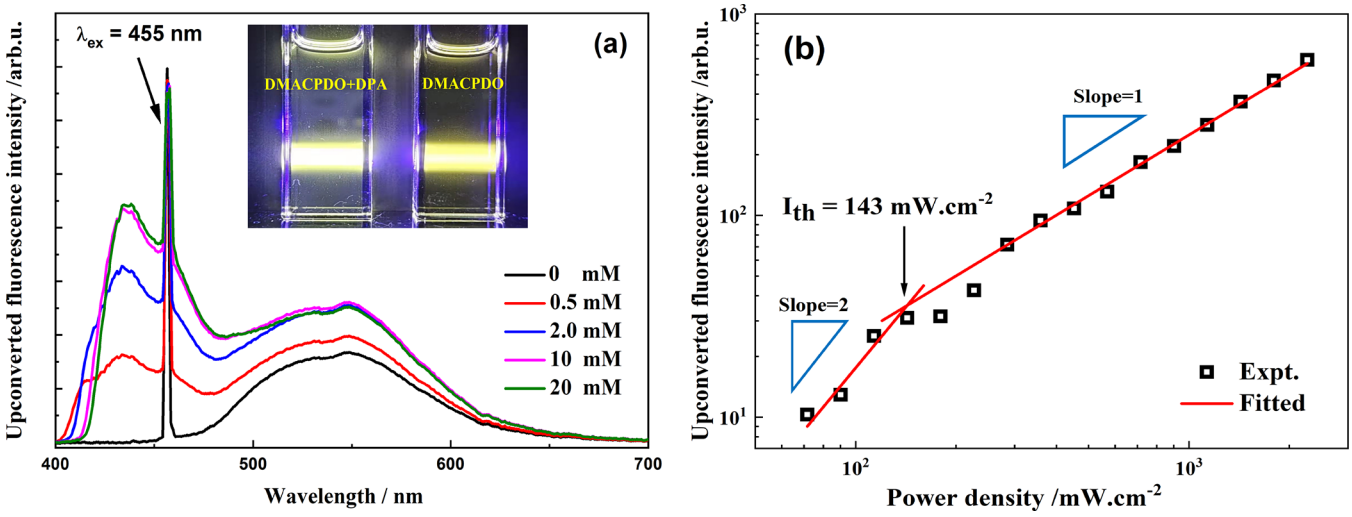

Figure 4. (a) Upconversion fluorescence emission spectra of DMACPDO (1 × 10^{-5} M) and DPA with various concentrations in deoxygenated toluene; room temperature and λ_{ex} = 455 nm. Insert: photos of the upconversion fluorescence of DMACPDO and DPA and the fluorescence of DMACPDO itself. (b) Double-logarithmic plot of the upconversion fluorescence intensity as a function of excitation power density; [DMACPDO] = 1 × 10^{-5} M and [DPA] = 10 mM.

https://doi.org/10.1021/acs.jpcc.2c07906
J. Phys. Chem. C 2023, 127, 2846−2854

Table 2. Quantum Yields of the Elementary Photophysical and Photochemical Processes Involved in the Present TTA Upconversion System in Deoxygenated Solutions at Room Temperature

solvent	Φ_{ISC} (%)	Φ_{RISC} (%)	Φ_{TTET} (%)	Φ_{FL}(DPA) (%)	Φ_{UC} (%)	Φ_{TTA} (%)
toluene	86	0.9	96	0.83 ± 0.03	22.3 ± 0.03	32.5
benzene	86	1.5	96	0.88 ± 0.03	21.9 ± 0.03	30.1
chlorobenzene	95	4.9	90	0.94 ± 0.03	8.1 ± 0.03	10.1

tration, which is attributed to reabsorption of DPA, the so-called "secondary inner filter effect", due to the overlap of upconversion fluorescence emission and sample absorption. In fact, this phenomenon is common in the visible-to-ultraviolet upconversion systems. Interestingly, almost unchanged peak intensity was observed at the DPA concentration of higher than 10 mM (purple and green curves in Figure 4a), thus suggesting an optimized DPA concentration of ∼10 mM for the present TTA upconversion system.

In Figure 4b, a double-logarithmic plot of the upconversion fluorescence intensity as a function of incident light power density is shown. A quadratic dependence on the excitation power at low intensities is observed, while the relationship is gradually shifted to a linear curve at higher intensity. This variation provides a solid evidence for the P-type delayed fluorescence.[45] In other words, the observed fluorescence of DPA in our experiments arises from the TTA upconversion mechanism. The threshold I_{th} was determined to be ∼143 mW cm^{-2} as the turning point in Figure 4b. In addition, the excitation power density was higher than I_{th} used in the upconversion experiments of Figure 4a.

Notably, both the remnant fluorescence of DMACPDO and the upconversion fluorescence of DPA were observed in the photoluminescence spectra of Figure 4a. Thus, a spectral fitting is necessary to precisely obtain the upconversion fluorescence component. Detailed information about the spectral fitting is described in the Supporting Information. The pure contribution by upconversion fluorescence of DPA in Figure 4a has been obtained precisely. Then, using the fluorescein as the standard (Φ_{std} = 90% in 0.1 M NaOH),[46] the upconversion quantum yield, Φ_{UC}, can be measured with eq 2

$$\Phi_{UC} = 2\Phi_{std}\left(\frac{A_{std}}{A_{sam}}\right)\left(\frac{I_{sam}}{I_{std}}\right)\left(\frac{\eta_{sam}}{\eta_{std}}\right)^2 \quad (2)$$

where A, I, and η are absorbance intensities, integrated luminescence intensities, and refractive indices of solvents used for the standard and samples. The equation is multiplied by a factor of 2 to make the maximum quantum yield to unity.[47] The Φ_{UC} values of the present system were determined to be 22.3% in toluene, 21.9% in benzene, and 8.1% in chlorobenzene. Additionally, taking the reabsorption of annihilator into account, the higher yield, the so-called the internal upconversion quantum yield ($\Phi_{UC,g}$), can be achieved, as suggested by Albinsson et al.[38] Notably, the quantum yields in toluene and benzene are higher than the maximal Φ_{UC} value (11.1%) predicted from the spin-statistic law in the TTA process. Similar high Φ_{UC} results were reported in some systems consisting of metal−organic[19,48] or BODIPY derivative photosensitizers.[4] We will try to explain the origin of such a significant solvent effect in Section 3.4.

In addition, there is an interesting phenomenon observed in current experiments. The remnant fluorescence of DMACPDO shows a positive correlation with the DPA concentration in toluene and benzene, but the opposite relationship in chlorobenzene, as shown in Figures 4a and S5. We know both RISC and nonradiation compete with the biomolecular TTET process for triplet DMACPDO. In toluene and benzene, the k_{RISC} values are apparently smaller than k_{NR}^{T}, as shown in Table S2, so that most of triplet population will be decayed without luminescence. However, with the addition of DPA, the TTET is significantly enhanced for decay of triplet DMACPDO. Consequently, most triplet sensitizers, especially those "dark" triplet (decay via nonradiation process instead of RISC), can contribute their energies to TTA upconversion fluorescence via efficient TTET and TTA processes. It is worth noting that the quantum yields of upconversion fluorescence in toluene and benzene are very high, and meanwhile, the upconversion fluorescence of DPA can be reabsorbed by DMACPDO according to the significant overlap between the DMACPDO absorption spectrum and the upconversion fluorescence of DPA. These factors facilitate the enhancement of remnant fluorescence intensity of DMACPDO, in addition to the increase of upconversion fluorescence, with increasing the DPA concentration.

In comparison, the opposite condition ($k_{RISC} \geq k_{NR}^{T}$) exists in chlorobenzene (Table S2). That means that the dominant decay pathway for the triplet DMACPDO is transferred back to the singlet state by RISC in the absence of DPA, leading to delayed fluorescence. Thus, with the addition of DPA, the TTET process can quickly reduce the triplet population and weaken delayed fluorescence intensity. Although the DMACPDO reabsorption of the TTA upconversion fluorescence also exists, the quantum yields of upconversion fluorescence and fluorescence emission of DMACPDO itself in chlorobenzene are much lower. Therefore, the remnant photofluorescence intensity is significantly reduced with the increase of DPA concentration.

3.4. TTA Upconversion Mechanism. As indicated in the Jablonski diagram (Figure 1), the Φ_{UC} value can be calculated according to eq 3

$$\Phi_{UC} = \Phi_{ISC}\Phi_{TTET}\Phi_{TTA}\Phi_{FL}(\mathrm{DPA}) \quad (3)$$

where Φ_{ISC} is the ISC efficiency, $\Phi_{ISC} = k_{ISC}/(k_{ISC} + k_{FL})$, and Φ_{TTA} and Φ_{FL}(DPA) are the TTA efficiency of ^{3}DPA* and the fluorescence emission quantum yield of ^{1}DPA*, respectively. In addition, the quantum yield of the RISC process, Φ_{RISC}, can be calculated by $\Phi_{RISC} = k_{RISC}/(k_{RISC} + k_{NR}^{T})$. Among the preceding equations, k_{ISC}, k_{RISC}, and k_{FL} are the rate constants of ISC, reverse ISC, and fluorescence emission of photosensitizer, respectively. Although the rate constants like k_{ISC}, k_{RISC}, and k_{NR}^{T} could not be directly measured in transient absorption spectroscopy experiments, we recently have built an explicit model for such TADF systems,[41] in which they can be derived from fitting the kinetics of delayed fluorescence. For DMACPDO, the obtained rate constants (k_{ISC}, k_{RISC}, k_{FL}, and k_{NR}^{T}) in the three solvents are listed in Table S2 of the Supporting Information. Accordingly, the quantum yields are calculated and summarized in Table 2.

https://doi.org/10.1021/acs.jpcc.2c07906
J. Phys. Chem. C 2023, 127, 2846−2854

Table 3. Calculated and Experimental Excitation Energies (in eV) of the Low-Lying Singlet and Triplet States of DPA in Three Solvents at Room Temperature

solvent	E_{S_1}	E_{T_1}	E_{T_2}	ΔE_{TTA}	$2E_{T_1} - E_{T_2}$	$E_{T_2} - E_{S_1}$
toluene	3.128,[a] 3.10,[b] 3.162[c]	1.736,[a] 1.72,[b] 1.734[c]	3.266,[a] 3.23,[b] 3.27[c]	0.345	0.206	0.139
benzene	3.129[a]	1.736[a]	3.266[a]	0.343	0.206	0.137
chlorobenzene	3.100[a]	1.737[a]	3.269[a]	0.373	0.205	0.168

[a]Present results, calculated at the B3LYP/6-31G(d) level. [b]Reference 50. [c]Reference 51.

Because the Φ_{ISC} and Φ_{TTET} values are high enough as shown in Table 2, the significant changes of Φ_{UC} observed in our experiments should arise from the TTA and/or the fluorescence emission of DPA processes. In our previous studies,[4] the fluorescence quantum yield (Φ_{FL}) of perylene (annihilator) shows a significant dependence on solvent polarity. Following this assumption, in the current solvents we also measured the fluorescence quantum yield of DPA itself, Φ_{FL}(DPA). As the Φ_{FL}(DPA) in benzene (0.88) was commonly accepted,[49] we used it as the standard and obtained this yield in the other two solvents according to the following equation: $\Phi_{FL}(\mathrm{DPA}) = \Phi_{std}\left(\frac{A_{std}}{A_{sam}}\right)\left(\frac{I_{sam}}{I_{std}}\right)\left(\frac{\eta_{sam}}{\eta_{std}}\right)^2$. The obtained Φ_{FL}(DPA) values are listed in Table 2, e.g., 0.83 in toluene and 0.94 in chlorobenzene. Considering these approximate Φ_{FL}(DPA) values, we excluded the fluorescence emission efficiency of annihilator from the critical factor for the Φ_{UC} difference.

Using the quantum yields of Φ_{ISC}, Φ_{TTET}, Φ_{FL}(DPA), and Φ_{UC} in Table 2, the experimental Φ_{TTA} value can be simply calculated according to eq 3, e.g., 0.325 in toluene, 0.301 in benzene, and 0.101 in chlorobenzene. It is worth noting that only Φ_{TTA} in chlorobenzene is lower than the maximal value (11.1%) calculated from the spin-statistics law, while the Φ_{TTA} data in toluene and benzene are much higher, strongly indicating that both quintet and triplet encounter complexes participate in the formation of the singlet excited DPA.[47]

As the TTA process proceeds in principle via the Dexter exchange mechanism, the viscosity of solvent and the energy gap ΔE_{TTA} (= $2E_{T_1} - E_{S_1}$) both might have significant influence, where E_{T1} and E_{S1} denote the energies of the lowest triplet and singlet states of DPA. The influence of solvent viscosity on the formation of triplet pair encounter (T_1T_1) can be roughly evaluated using diffusion rates. As shown in Table 1, the calculated $k_{diffuse}$ values are moderately changed from 11.3×10^9 M^{-1} s^{-1} in toluene and 11.1×10^9 M^{-1} s^{-1} in benzene to 8.3×10^9 M^{-1} s^{-1} in chlorobenzene. Interestingly, this sequence is generally consistent with the Φ_{TTA} values, but the quantitative difference is quite large. For example, the Φ_{TTA} values in toluene and benzene are ca. 2.75 times higher than that in chlorobenzene, but there is only a 1.35-fold increase for the $k_{diffuse}$ values. The direct comparison clearly indicates that the viscosity of solvent may play a considerable role but is not the determinant factor. Notably, as suggested by Yokoyama et al.,[40] an increase of solvent viscosity can slow down molecular rotation and promote spin relaxation in the (T_1T_1) encounter, thus leading to an enhancement on TTA yield. Obviously, this action mechanism is just opposite to our experimental results. Thus, the Φ_{TTA} difference in Table 2 cannot come from the influence of solvent viscosity.

According to the principle of resonance energy transfer, an ideal ΔE_{TTA} for favorable TTA process is positive but close to zero. We calculated the energies of the low-lying singlet and triplet states of DPA using the B3LYP/6-31G(d) and time-dependent B3LYP methods. Table 3 lists the present calculated data as well as previous calculated results.[50,51] Apparently, for the S_1, T_1, and T_2 states, a general agreement is obtained for these calculated excitation energies, e.g., E_{S_1} = 3.10−3.13 eV, E_{T_1} = 1.74 eV, and E_{T_2} = 3.27 eV. In contrast, the experimental E_{S_1}(DPA) data can be precisely determined to be 3.08 eV from the absorption and fluorescence emission spectra of DPA, using the strategy suggested by Vandewal et al.[52] Meanwhile, the experimentally reported E_{T_1}(DPA) is 1.77 eV in aromatic hydrocarbon solvents like toluene and benzene.[36,49,53−55] These experimental values are greatly consistent with our calculated data, as shown in Table 3. Additionally, the dominant electronic transitions for the S_1 and T_1 states are both the HOMO → LUMO localized excitation with more than 94%. Because the HOMO and LUMO are both located at the central anthracene unit, it is reasonable that no significant solvent effect exists on the E_{S_1} and E_{T_1} energies of DPA. Using these calculated energies, positive ΔE_{TTA} values are theoretically predicted as shown in Table 3, indicative of a feasible TTA process. Interestingly, a higher ΔE_{TTA} of 0.373 eV in chlorobenzene is achieved than those in toluene and benzene (~0.345 eV), which provides a probable explanation for the lowest Φ_{TTA} value in chlorobenzene.

According to the initial spin states of annihilator, the formed complex of triplet pair (T_1T_1) can be of singlet, triplet, or quintet multiplicity:

$$T_1 + T_1 \rightleftharpoons {}^1(T_1T_1) \rightarrow S_1 + S_0 \quad (4)$$

$$\rightleftharpoons {}^3(T_1T_1) \rightarrow T_2 + S_0 \xrightarrow{IC} T_1 + S_0 \quad (5)$$

$$\rightleftharpoons {}^5(T_1T_1) \not\rightarrow Q_1 + S_0 \quad (6)$$

Based on spin statistics with the strong coupling limit, the singlet complex $^1(T_1T_1)$ can be formed with a probability of 1/9, while triplet $^3(T_1T_1)$ and quintet $^5(T_1T_1)$ ones are produced with the probabilities of 3/9 and 5/9, respectively. It is worth noting that only pathway (4) can produce the desired singlet excited state to emit upconversion fluorescence, which causes the common maximal Φ_{TTA} value (1/9 = 11.1%). However, as pathway (6) to form a quintet excited state (Q_1) is highly endothermic, the quintet complex $^5(T_1T_1)$ usually will dissociates into two T_1. Meanwhile, when $E(T_2)$ is lower than twice $E(T_1)$, pathway (5) is exothermic, and the TTA quantum yield may reach a limit of 40% as the product T_2 can fast decay to T_1 by internal conversion. Notably, the experimental Φ_{TTA} values in toluene and benzene are close to this upper limit (Table 2), especially when the $\Phi_{UC,g}$ values are used to eliminate the secondary inner filter effect. Consequently, the contribution from the pathway (5) is believed to play determinant role on the TTA process in the current solutions.

https://doi.org/10.1021/acs.jpcc.2c07906
J. Phys. Chem. C 2023, 127, 2846−2854

Using the calculated data of E_{T_1} and E_{T_2} in Table 3, a positive ΔE (= $2E_{T_1} - E_{T_2}$) value is achieved, indicating a feasible TTA mechanism involving pathway (5). However, the calculated $2E_{T_1} - E_{T_2}$ values are almost equivalent as 0.205 and 0.206 eV, and thus the contribution of pathway (5) should be approximately identical in the three solvents. In contrast, we notice that in Table 3 a positive value of $E_{T_2} - E_{S_1}$ exists for DPA in all solvents, and moreover, such small data of 0.137−0.168 eV indicate another near-resonance ISC from T_2 directly to S_1, as

$$T_1 + T_1 \rightleftharpoons {}^3(T_1T_1) \rightarrow T_2 + S_0 \xrightarrow{ISC} S_1 + S_0 \quad (7)$$

As the ISC rate strongly depends on the energy difference of $E_{T_2} - E_{S_1}$, we can imagine that with the near-resonance conditions the ISC yield from T_2 to S_1 will be significantly enhanced, like in toluene and benzene. Notably, this process shows a new mechanism to improve the upper limit of Φ_{TTA} to 100%. In the TTA of DPA process in toluene and benzene, pathway (7) might play a pivotal role.

It should be added that a complicated contribution of charge-transfer characteristic is found for the T_2 state in our calculation, as the HOMO−2 → LUMO (33%), HOMO → LUMO+6 (25%), and HOMO−6 → LUMO (23%), where the HOMO−2 and HOMO−6 are degenerated. Unlike the HOMO and LUMO located at the anthracene unit, the HOMO−2, HOMO−6, and LUMO+6 are dispersed throughout the whole molecule. Thus, B3LYP (or time-dependent DFT) as a single-reference DFT-based approach might be not well suited to the T_2 calculation. Therefore, to precisely determine the T_2 energy, it is necessary to perform a multireference configuration interaction calculation like the CASSCF or CASPT2 levels, which is beyond the scope of this paper due to too high cost. Despite this, we can still affirm that the polarity of solvent plays the most important role in the overall TTA upconversion of the DMACPDO/DPA system by adjusting the higher triplet energy.

4. CONCLUSIONS

According to the long-lived triplet state and high molar extinction coefficient, TADF molecules are potential heavy-atom-free organic photosensitizers for TTA upconversion. In this work, we conducted a new TTA upoconversion system involved a recently reported TADF molecule, DMACPDO, as triplet photosensitizer and DPA as annihilator. Using transient absorption and fluorescence spectroscopy, we experimentally investigated its performance in three common solvents: toluene, benzene, and chlorobenzene. The highly efficient TTA upconversion fluorescence emission of DPA was clearly observed, with the Φ_{UC} values of 22.3%, 21.9%, and 8.1% in toluene, benzene, and chlorobenzene, respectively.

Based on the measured dynamics rate constants of DMACPDO and fluorescence quantum yield of DPA, the solvent effect on the ISC and TTET processes was discussed. The viscosity of solvent has a certain influence but is not the determinant factor for the bimolecular TTET dynamics. In contrast, the ultrahigh Φ_{TTA} and Φ_{UC} values in toluene and benzene strongly imply the participation of triplet encounter complexes in the direct and indirect formation of the singlet excited DPA. On the basis of the calculated excitation energies for the S_1, T_1, and T_2 states of DPA, we proposed that the polarity of solvent plays the most important role in the TTA upconversion process by adjusting the higher triplet energy. In summary, this is a representative example for application of a TADF molecule as heavy-atom-free triplet photosensitizer, and our conclusions provide more clues to an in-depth understanding of the complex solvent effect in the similar TTA upconversion system.

■ ASSOCIATED CONTENT

Supporting Information

The Supporting Information is available free of charge at https://pubs.acs.org/doi/10.1021/acs.jpcc.2c07906.

Detailed information for the steady-state UV−vis absorption spectra, fluorescence emission kinetics, TTA upconversion fluorescence emission spectra, spectral fitting and Cartesian coordinates of the optimized geometries of DPA in ground state at the B3LYP/6-31G(d) level (PDF)

■ AUTHOR INFORMATION

Corresponding Authors

Yaxiong Wei − *School of Physics and Electronic Information, Anhui Normal University, Wuhu, Anhui 241000, China*; Email: davidl@mail.ustc.edu.cn

Lin Chen − *School of Physics and Materials Engineering, Hefei Normal University, Hefei, Anhui 230601, China*; Email: chenlin@hfnu.edu.cn

Xiaoguo Zhou − *Hefei National Laboratory for Physical Sciences at the Microscale, Department of Chemical Physics, University of Science and Technology of China, Hefei, Anhui 230026, China*; orcid.org/0000-0002-0264-0146; Email: xzhou@ustc.edu.cn

Authors

Min Zheng − *Hefei National Laboratory for Physical Sciences at the Microscale, Department of Chemical Physics, University of Science and Technology of China, Hefei, Anhui 230026, China*

Yuanming Li − *Hefei National Laboratory for Physical Sciences at the Microscale, Department of Chemical Physics, University of Science and Technology of China, Hefei, Anhui 230026, China*

Shilin Liu − *Hefei National Laboratory for Physical Sciences at the Microscale, Department of Chemical Physics, University of Science and Technology of China, Hefei, Anhui 230026, China*

Complete contact information is available at: https://pubs.acs.org/10.1021/acs.jpcc.2c07906

Author Contributions

M.Z.: measured spectra, performed theoretical calculation, and wrote original draft. Y.L.: performed data curation. S.L. and X.Z.: provided funding. Y.W., L.C., and X.Z.: conceived the idea, led the project, provided funding, and wrote and reviewed the draft.

Notes

The authors declare no competing financial interest.

■ ACKNOWLEDGMENTS

This work was financially supported by the National Natural Science Foundation of China (Nos. 21873089, 22203004, and 22073088). L.C. is also grateful for the financial support of the

Educational Commission of Anhui Province of China (No. KJ2018A0491).

REFERENCES

(1) Parker, C. A.; Hatchard, C. G. Delayed Fluorescence from Solutions of Anthracene and Phenanthrene. *Proc. R. Soc. London. Series A, Mathematical and Physical Sciences* **1962**, *269*, 574−584.
(2) Askes, S. H. C.; Bahreman, A.; Bonnet, S. Activation of a Photodissociative Ruthenium Complex by Triplet−Triplet Annihilation Upconversion in Liposomes. *Angew. Chem., Int. Ed.* **2014**, *53*, 1029−1033.
(3) Fan, C.; Wu, W.; Chruma, J. J.; Zhao, J.; Yang, C. Enhanced Triplet−Triplet Energy Transfer and Upconversion Fluorescence through Host−Guest Complexation. *J. Am. Chem. Soc.* **2016**, *138*, 15405−15412.
(4) Zhou, Q.; Zhou, M.; Wei, Y.; Zhou, X.; Liu, S.; Zhang, S.; Zhang, B. Solvent effects on the triplet−triplet annihilation upconversion of diiodo-Bodipy and perylene. *Phys. Chem. Chem. Phys.* **2017**, *19*, 1516−1525.
(5) Wei, Y.; Zhou, M.; Zhou, Q.; Zhou, X.; Liu, S.; Zhang, S.; Zhang, B. Triplet−triplet annihilation upconversion kinetics of C60−Bodipy dyads as organic triplet photosensitizers. *Phys. Chem. Chem. Phys.* **2017**, *19*, 22049−22060.
(6) Wei, Y.; Zheng, M.; Zhou, Q.; Zhou, X.; Liu, S. Application of a bodipy−C70 dyad in triplet−triplet annihilation upconversion of perylene as a metal-free photosensitizer. *Org. Biomol. Chem.* **2018**, *16*, 5598−5608.
(7) Wei, Y.; Zheng, M.; Chen, L.; Zhou, X.; Liu, S. Near-infrared to violet triplet−triplet annihilation fluorescence upconversion of Os(ii) complexes by strong spin-forbidden transition. *Dalton Trans.* **2019**, *48*, 11763−11771.
(8) Wei, Y.; Li, Y.; Zheng, M.; Zhou, X.; Zou, Y.; Yang, C. Simultaneously High Upconversion Efficiency and Large Anti-Stokes Shift by Using Os(II) Complex Dyad as Triplet Photosensitizer. *Adv. Opt. Mater.* **2020**, *8*, 1902157.
(9) Cheng, Y. Y.; Fückel, B.; MacQueen, R. W.; Khoury, T.; Clady, R. G. C. R.; Schulze, T. F.; Ekins-Daukes, N. J.; Crossley, M. J.; Stannowski, B.; Lips, K.; et al. Improving the light-harvesting of amorphous silicon solar cells with photochemical upconversion. *Energy Environ. Sci.* **2012**, *5*, 6953−6959.
(10) Nattestad, A.; Cheng, Y. Y.; MacQueen, R. W.; Schulze, T. F.; Thompson, F. W.; Mozer, A. J.; Fückel, B.; Khoury, T.; Crossley, M. J.; Lips, K.; et al. Dye-Sensitized Solar Cell with Integrated Triplet−Triplet Annihilation Upconversion System. *J. Phys. Chem. Lett.* **2013**, *4*, 2073−2078.
(11) Gray, V.; Dzebo, D.; Abrahamsson, M.; Albinsson, B.; Moth-Poulsen, K. Triplet−triplet annihilation photon-upconversion: towards solar energy applications. *Phys. Chem. Chem. Phys.* **2014**, *16*, 10345−10352.
(12) Huang, L.; Cui, X.; Therrien, B.; Zhao, J. Energy-Funneling-Based Broadband Visible-Light-Absorbing Bodipy−C60 Triads and Tetrads as Dual Functional Heavy-Atom-Free Organic Triplet Photosensitizers for Photocatalytic Organic Reactions. *Chem.—Eur. J.* **2013**, *19*, 17472−17482.
(13) Zhao, J.; Wu, W.; Sun, J.; Guo, S. Triplet photosensitizers: from molecular design to applications. *Chem. Soc. Rev.* **2013**, *42*, 5323−5351.
(14) Liu, Y.; Su, Q.; Zou, X.; Chen, M.; Feng, W.; Shi, Y.; Li, F. Near-infrared in vivo bioimaging using a molecular upconversion probe. *Chem. Commun.* **2016**, *52*, 7466−7469.
(15) Tian, B.; Wang, Q.; Su, Q.; Feng, W.; Li, F. In vivo biodistribution and toxicity assessment of triplet-triplet annihilation-based upconversion nanocapsules. *Biomaterials* **2017**, *112*, 10−19.
(16) Xu, M.; Zou, X.; Su, Q.; Yuan, W.; Cao, C.; Wang, Q.; Zhu, X.; Feng, W.; Li, F. Ratiometric nanothermometer in vivo based on triplet sensitized upconversion. *Nat. Commun.* **2018**, *9*, 2698.
(17) Cakmak, Y.; Kolemen, S.; Duman, S.; Dede, Y.; Dolen, Y.; Kilic, B.; Kostereli, Z.; Yildirim, L. T.; Dogan, A. L.; Guc, D.; et al. Designing Excited States: Theory-Guided Access to Efficient Photosensitizers for Photodynamic Action. *Angew. Chem., Int. Ed.* **2011**, *50*, 11937−11941.
(18) Erbas, S.; Gorgulu, A.; Kocakusakogullari, M.; Akkaya, E. U. Non-covalent functionalized SWNTs as delivery agents for novel Bodipy-based potential PDT sensitizers. *Chem. Commun.* **2009**, 4956−4958.
(19) Zhao, J.; Ji, S.; Guo, H. Triplet−triplet annihilation based upconversion: from triplet sensitizers and triplet acceptors to upconversion quantum yields. *RSC Adv.* **2011**, *1*, 937−950.
(20) Islangulov, R. R.; Kozlov, D. V.; Castellano, F. N. Low power upconversion using MLCT sensitizers. *Chem. Commun.* **2005**, 3776−3778.
(21) Baluschev, S.; Miteva, T.; Yakutkin, V.; Nelles, G.; Yasuda, A.; Wegner, G. Up-Conversion Fluorescence: Noncoherent Excitation by Sunlight. *Phys. Rev. Lett.* **2006**, *97*, 143903.
(22) Zhao, W.; Castellano, F. N. Upconverted Emission from Pyrene and Di-tert-butylpyrene Using Ir(ppy)3 as Triplet Sensitizer. *J. Phys. Chem. A* **2006**, *110*, 11440−11445.
(23) Baluschev, S.; Yakutkin, V.; Miteva, T.; Avlasevich, Y.; Chernov, S.; Aleshchenkov, S.; Nelles, G.; Cheprakov, A.; Yasuda, A.; Müllen, K.; et al. Blue-Green Up-Conversion: Noncoherent Excitation by NIR Light. *Angew. Chem., Int. Ed.* **2007**, *46*, 7693−7696.
(24) Monguzzi, A.; Tubino, R.; Meinardi, F. Upconversion-induced delayed fluorescence in multicomponent organic systems: Role of Dexter energy transfer. *Phys. Rev. B* **2008**, *77*, 155122.
(25) Singh-Rachford, T. N.; Castellano, F. N. Pd(II) Phthalocyanine-Sensitized Triplet−Triplet Annihilation from Rubrene. *J. Phys. Chem. A* **2008**, *112*, 3550−3556.
(26) Chen, H.-C.; Hung, C.-Y.; Wang, K.-H.; Chen, H.-L.; Fann, W. S.; Chien, F.-C.; Chen, P.; Chow, T. J.; Hsu, C.-P.; Sun, S.-S. White-light emission from an upconverted emission with an organic triplet sensitizer. *Chem. Commun.* **2009**, 4064−4066.
(27) Wu, W.; Guo, H.; Wu, W.; Ji, S.; Zhao, J. Organic Triplet Sensitizer Library Derived from a Single Chromophore (BODIPY) with Long-Lived Triplet Excited State for Triplet−Triplet Annihilation Based Upconversion. *Journal of Organic Chemistry* **2011**, *76*, 7056−7064.
(28) Chen, Y.; Zhao, J.; Xie, L.; Guo, H.; Li, Q. Thienyl-substituted BODIPYs with strong visible light-absorption and long-lived triplet excited states as organic triplet sensitizers for triplet−triplet annihilation upconversion. *RSC Adv.* **2012**, *2*, 3942−3953.
(29) Guo, S.; Wu, W.; Guo, H.; Zhao, J. Room-Temperature Long-Lived Triplet Excited States of Naphthalenediimides and Their Applications as Organic Triplet Photosensitizers for Photooxidation and Triplet−Triplet Annihilation Upconversions. *Journal of Organic Chemistry* **2012**, *77*, 3933−3943.
(30) Wu, W.; Liu, L.; Cui, X.; Zhang, C.; Zhao, J. Red-light-absorbing diimine Pt(ii) bisacetylide complexes showing near-IR phosphorescence and long-lived 3IL excited state of Bodipy for application in triplet−triplet annihilation upconversion. *Dalton Trans.* **2013**, *42*, 14374−14379.
(31) Uoyama, H.; Goushi, K.; Shizu, K.; Nomura, H.; Adachi, C. Highly efficient organic light-emitting diodes from delayed fluorescence. *Nature* **2012**, *492*, 234−238.
(32) Wu, T. C.; Congreve, D. N.; Baldo, M. A. Solid state photon upconversion utilizing thermally activated delayed fluorescence molecules as triplet sensitizer. *Appl. Phys. Lett.* **2015**, *107*, 031103.
(33) Peng, J.; Guo, X.; Jiang, X.; Zhao, D.; Ma, Y. Developing efficient heavy-atom-free photosensitizers applicable to TTA upconversion in polymer films. *Chem. Sci.* **2016**, *7*, 1233−1237.
(34) Wei, D.; Ni, F.; Zhu, Z.; Zou, Y.; Yang, C. A red thermally activated delayed fluorescence material as a triplet sensitizer for triplet−triplet annihilation up-conversion with high efficiency and low energy loss. *J. Mater. Chem. C* **2017**, *5*, 12674−12677.
(35) Yanai, N.; Kozue, M.; Amemori, S.; Kabe, R.; Adachi, C.; Kimizuka, N. Increased vis-to-UV upconversion performance by energy level matching between a TADF donor and high triplet energy acceptors. *J. Mater. Chem. C* **2016**, *4*, 6447−6451.

https://doi.org/10.1021/acs.jpcc.2c07906
J. Phys. Chem. C 2023, 127, 2846−2854

(36) Chen, W.; Song, F.; Tang, S.; Hong, G.; Wu, Y.; Peng, X. Red-to-blue photon up-conversion with high efficiency based on a TADF fluorescein derivative. *Chem. Commun.* **2019**, *55*, 4375−4378.
(37) Wei, Y.; Pan, K.; Cao, X.; Li, Y.; Zhou, X.; Yang, C. Multiple Resonance Thermally Activated Delayed Fluorescence Sensitizers Enable Green-to-Ultraviolet Photon Upconversion: Application in Photochemical Transformations. *CCS Chem.* **2022**, *4*, 3852.
(38) Olesund, A.; Johnsson, J.; Edhborg, F.; Ghasemi, S.; Moth-Poulsen, K.; Albinsson, B. Approaching the Spin-Statistical Limit in Visible-to-Ultraviolet Photon Upconversion. *J. Am. Chem. Soc.* **2022**, *144*, 3706−3716.
(39) Zhou, Y.; Liu, Y.-H.; Rahman, S. N.; Hall, D.; Sham, L. J.; Lo, Y.-H. Discovery of a photoresponse amplification mechanism in compensated PN junctions. *Appl. Phys. Lett.* **2015**, *106*, 031103.
(40) Yokoyama, K.; Wakikawa, Y.; Miura, T.; Fujimori, J.-i.; Ito, F.; Ikoma, T. Solvent Viscosity Effect on Triplet−Triplet Pair in Triplet Fusion. *J. Phys. Chem. B* **2015**, *119*, 15901−15908.
(41) Zheng, M.; Li, Y.; Wei, Y.; Chen, L.; Zhou, X.; Liu, S. Determining the Energy Gap between the S1 and T1 States of Thermally Activated Delayed Fluorescence Molecular Systems Using Transient Fluorescence Spectroscopy. *J. Phys. Chem. Lett.* **2022**, *13*, 2507−2515.
(42) Wu, K.; Zhang, T.; Wang, Z.; Wang, L.; Zhan, L.; Gong, S.; Zhong, C.; Lu, Z.-H.; Zhang, S.; Yang, C. De Novo Design of Excited-State Intramolecular Proton Transfer Emitters via a Thermally Activated Delayed Fluorescence Channel. *J. Am. Chem. Soc.* **2018**, *140*, 8877−8886.
(43) Liu, X.; Chen, L.; Zhou, Q.; Zhou, X.; Liu, S. Electron transfer reactions between 1,8-dihydroxyanthraquinone and pyrimidines: A laser flash photolysis study. *J. Photochem. Photobiol., A* **2013**, *269*, 42−48.
(44) Chen, L.; Zhou, Q.; Liu, X.; Zhou, X.; Liu, S. Solvent Effect on the Photoinduced Electron Transfer Reaction Between Thioxanthen-9-one and Diphenylamine. *Chin. J. Chem. Phys.* **2015**, *28*, 493−500.
(45) Haefele, A.; Blumhoff, J.; Khnayzer, R. S.; Castellano, F. N. Getting to the (Square) Root of the Problem: How to Make Noncoherent Pumped Upconversion Linear. *J. Phys. Chem. Lett.* **2012**, *3*, 299−303.
(46) Olmsted, J. Calorimetric determinations of absolute fluorescence quantum yields. *J. Phys. Chem.* **1979**, *83*, 2581−2584.
(47) Singh-Rachford, T. N.; Castellano, F. N. Photon upconversion based on sensitized triplet−triplet annihilation. *Coord. Chem. Rev.* **2010**, *254*, 2560−2573.
(48) Guo, H.; Li, Q.; Ma, L.; Zhao, J. Fluorene as π-conjugation linker in N∧N Pt(ii) bisacetylide complexes and their applications for triplet−triplet annihilation based upconversion. *J. Mater. Chem.* **2012**, *22*, 15757−15768.
(49) Suzuki, T.; Nagano, M.; Watanabe, S.; Ichimura, T. Study of the photophysics and energy transfer of 9,10-diphenylanthracene in solution. *J. Photochem. Photobiol., A* **2000**, *136*, 7−13.
(50) Gray, V.; Dzebo, D.; Lundin, A.; Alborzpour, J.; Abrahamsson, M.; Albinsson, B.; Moth-Poulsen, K. Photophysical characterization of the 9,10-disubstituted anthracene chromophore and its applications in triplet−triplet annihilation photon upconversion. *J. Mater. Chem. C* **2015**, *3*, 11111−11121.
(51) Ieuji, R.; Goushi, K.; Adachi, C. Triplet−triplet upconversion enhanced by spin−orbit coupling in organic light-emitting diodes. *Nat. Commun.* **2019**, *10*, 5283.
(52) Vandewal, K.; Benduhn, J.; Nikolis, V. C. How to determine optical gaps and voltage losses in organic photovoltaic materials. *Sustainable Energy Fuels* **2018**, *2*, 538−544.
(53) Han, J.; Jiang, Y.; Obolda, A.; Duan, P.; Li, F.; Liu, M. Doublet−Triplet Energy Transfer-Dominated Photon Upconversion. *J. Phys. Chem. Lett.* **2017**, *8*, 5865−5870.
(54) Hasegawa, R.; Iwakiri, S.; Kubo, Y. Synthesis and triplet sensitization of bis(arylselanyl)BOPHYs; potential application in triplet−triplet annihilation upconversion. *New J. Chem.* **2021**, *45*, 6091−6099.
(55) Huang, Z.; Li, X.; Mahboub, M.; Hanson, K. M.; Nichols, V. M.; Le, H.; Tang, M. L.; Bardeen, C. J. Hybrid Molecule−Nanocrystal Photon Upconversion Across the Visible and Near-Infrared. *Nano Lett.* **2015**, *15*, 5552−5557.

https://doi.org/10.1021/acs.jpcc.2c07906
J. Phys. Chem. C 2023, 127, 2846−2854